THE OPTICS OF THE OWL 100-M ADAPTIVE TELESCOPE

P. Dierickx, J. Beletic, B. Delabre, M. Ferrari, R. Gilmozzi, N. Hubin
European Southern Observatory

Abstract

The optical design of the OWL 100-m class visible and near-infrared telescope, with integrated adaptive optics, departs substantially from classical two-mirror solutions. We propose using spherical shapes for the primary and secondary mirrors due to manufacturing, performance and cost constraints. The optical prescription must balance conflicting constraints such as the design of the telescope structure, the constraints set by adaptive tomography correction, and the feasibility of the corrective optics which compensates for the spherical and field aberrations of the primary-secondary mirrors. The number of mirrors, larger than in classical 2-mirror designs, implies additional variables. Within the limits set by the feasibility of optical testing of the aspheric surfaces, we present two optical designs for the telescope and derive high level requirements on active and adaptive control.

Keywords OWL, Extremely Large Telescope, Optical Design, active optics, adaptive optics, segmented optics, optical fabrication, optical testing.

1. Introduction

The preliminary top level requirements underlying the optical design of the OWL 100-m class telescope are outlined in Table 1. OWL is basically defined as a 100-m class telescope providing diffraction-limited angular resolution in the visible and near-infrared. The telescope is to be normally operated with atmospheric turbulence compensation. However, a certain range of science objectives, e.g. wide-field, low-resolution 3D spectroscopy (telescope "searcher" mode, providing extended targets for further scrutiny at high resolution), do not require compensation of atmospheric turbulence. In this mode, the telescope must deliver seeing-limited images.

In order to achieve adaptive correction in the visible with $r_0 \approx 20$ cm, adaptive mirrors will have to accommodate up to about 500,000 actuators. Infrared systems at ~1 and ~2 microns respectively require 4 and 16 times less actuators, but they will have to cover a proportionally larger field of view. At this stage, however, the required number of specific adaptive systems is unclear. There are arguments, on the telescope side, to keep aerial density of actuators at the level required in the visible or near-infrared.

	Requirement	Goal
Collecting area (filled aperture)	≥ 6,000 m^2	≥ 7,000 m^2
Science field of view (diameter)	2 arc min. (IR)	3 arc min.
	30 arc secs (Visible)	1 arc min.
Wavelength range Imaging	0.35 to 2.5 microns	
Spectroscopy	0.35 to 12.5 microns	
Strehl ratio (at 0.5 microns)	≥ 0.20	≥ 0.40
Angular resolution in adaptive mode	Diffraction-limited (100-m diameter aperture)	
Angular resolution in non-adaptive mode	Seeing-limited (best seeing 0.4 arc secs)	
Sky coverage	TBD	Maximize

Table 1. OWL preliminary top level requirements

In adaptive mode, proper sampling of the PSF in the visible implies a final focal ratio of ~f/60 with a pixel size of 15 μm. It must be observed that, however small it may seem in terms of sky area, the field of view exceeds that of almost any telescope ever built, in terms of data points. Indeed, a 30×30 arc sec^2 diffraction-limited field of view corresponds to at least 30 GB of data.

As far as the optical design is concerned, the dimensioning requirements are essentially the pupil size, and multi-conjugate adaptive optics with natural guide stars.

The first consideration is the sheer size of the

Submitted at the *Workshop on Extremely Large Telescopes*, Bäckaskog, Sweden, June 1-2, 1999.

pupil, which implies segmentation. Cost and fabrication constraints, in turn, imply that strong preference is given to solutions for which the largest primary and secondary mirrors can be made of identical, mass-produced segments. Furthermore, the strategy followed in the feasibility assessment of OWL requires that, to the maximum possible extent, preference be given to proven solutions or, failing that, to solutions which require minimum extrapolation from proven ones. Therefore, unless a competitive optical fabrication process for mass-fabrication of off-axis aspheric segments could be demonstrated, the design must accommodate a spherical primary mirror, whose segments could be mass-produced by replication or polishing on planetary machines. Furthermore, it should be noted that an aspheric primary would not necessarily lead to better quality and larger field of view. Indeed, one of the designs presented here has better performance than an equivalent Ritchey-Chrétien over the science field.

The focal ratio of the primary mirror determines the structure length and must be minimized for structural reasons (a siderostat design would alleviate this constraint, at the expense of sky coverage, complex segmentation patterns, and substantially higher costs). A fast primary mirror, in turn, implies strong spherical and field aberrations, and highly aspheric corrective optics. The lower limit will be set by field, fabrication, and baffling constraints. The upper limit is derived from (very) preliminary designs of the mechanical structure; current estimate of the maximum distance to secondary is130-m.

A prime focus with corrector configuration would, in view of the maximum structure height, imply a ~f/1.30 primary. No acceptable solution has been found so far to accommodate such fast focal ratio. In addition to field limitation and a severe straylight issue, the correction of the spherical aberration, whose amplitude increases with the inverse fourth power of the focal ratio, becomes prohibitively difficult. A possible solution is a folded prime focus with corrector, which allows a relaxation of the focal ratio of the primary mirror, at the cost of a very large flat secondary mirror. One of the designs proposed here is based on that principle.

The shape of the secondary mirror is determined by design and feasibility considerations. First, in a Dall-Kirkham solution with aspheric secondary mirror, the extremely large coma term implies an unacceptably small field of view. Second, there does not seem to be any satisfactory solution to the optical testing of a very large, highly aspheric convex mirror. Finally, the secondary mirror must be far from the caustic of spherical aberration of the primary mirror. This will, eventually, imply large size and segmentation.

At this point, we conclude that the pupil size implies spherical, segmented primary and secondary mirrors, the defining engineering constraint being mass-production of the primary mirror segment. The reasoning is summarized in Fig. 1.

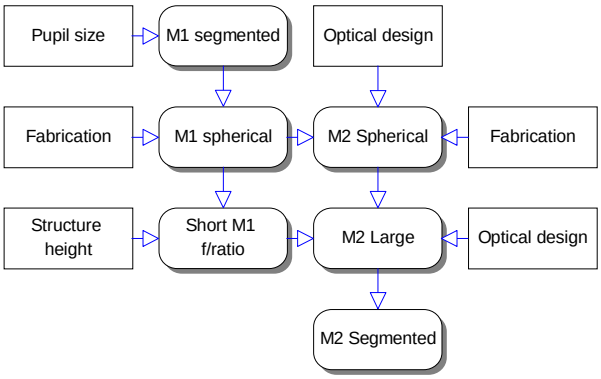

Figure 1 Design considerations, primary and secondary mirrors

A corrective optical system must be implemented to cancel spherical aberration and provide sufficient field of view for science applications and active and adaptive control. Two solutions have been derived so far, and will be explained in section 3.

The second consideration is multi-conjugate adaptive optics, which implies that adaptive mirrors be conjugate to the turbulent layers. Hence, the optical solution must provide real images of atmospheric layers at convenient locations and magnifications. Note that the numerical aperture of the conjugation layer-mirror is, in the object space, equal to the field of view (in radians). The highest resolution, at the level of the atmospheric layer, will therefore be λ/α, where λ is the wavelength and α the angular field radius. In the visible and with a field radius of 15 arc seconds, we obtain a spatial resolution of 7 mm in the turbulent layers, i.e. a conveniently small fraction of the atmospheric coherence length r_0. This resolution will be degraded by the aberrations of the conjugation but, as numerical apertures are very small, the dominant aberration will likely be distortion.

Adaptive mirror technology will evidently be strongly dimensioning. Optical design considerations would require the adaptive mirrors to be as large as possible, but there is, as of today, little basis to make rigorous projections as to maximum diameter. We tentatively assume that adaptive mirrors would be in the 0.5 to 2-m range.

Assuming adaptive control with natural stars, the telescope must provide sufficient field of view to ensure maximum sky coverage. The actual field of view of the telescope is therefore larger than the science field, and we define a *technical field*,

where optical quality should not degrade the accuracy of wavefront sensing i.e. wavefront accuracy in the technical field must be a fraction of the atmospheric phase excursion. Preliminary analysis predicts that a minimum field of view of 10 arc minutes diameter is required to achieve reasonable sky coverage.

Closed-loop adaptive optics requires that the beam corresponding to the guide star follows nearly the same path as the science beam. Transferring the entire technical field through the adaptive module would imply prohibitively large and complex relay optics and adaptive mirrors. The solution currently envisaged is to implement image transport. The guide star would be selected in the technical field, and relocated by an optical trombone close to the science field. The beam would have to be tilted to illuminate the appropriate sections of the adaptive mirrors. This solution is still to be evaluated for its impact in terms of residual errors and requirements for the image transport and layout of the adaptive optical train.

It is not entirely clear, however, that tomographic correction imperatively requires a closed-loop scheme.

The overall principle of the telescope optical system is shown in Fig. 2. In the following, mirrors will be numbered M1, …, M_N, in the same sequence as that of the reflection of the light beams. We define a *technical field*, located before the adaptive modules, substantially larger than the science field, and used by active and adaptive sensors.

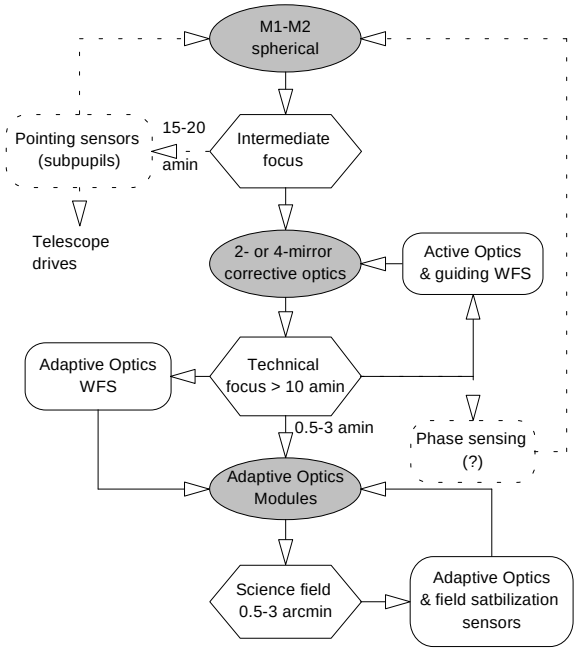

Figure 2 Optical principle
(all fields are diameters)

Active optics is integrated into the corrector. The latter is made of at least two large, flexible monolithic mirrors. Active control will likely require several guide stars to allow reconstruction of the optical prescription and closed-loop control.

Finally, the intermediate focus of the pair M1-M2 might be usable for pointing segments coarse alignment, and centering of the corrector. The general principle is to define a set of conveniently located sub-pupils, in the range of 50-100 cm diameter, and use images of off-axis stars to set the pointing of the telescope and possibly the alignment of the segments. One of the two designs presented in this article does not, however, provide a suitable intermediate focus.

2. Optical quality requirement

The optical concept calls for a system providing seeing-limited performance at the technical focus and diffraction-limited performance at the science focus, atmospheric turbulence being set aside. Telescope and turbulence contributions are tentatively split is as follows:

- Loss of Strehl Ratio associated with all error sources except atmospheric turbulence ≤ 30% (goal ≤ 20%);
- Loss of Strehl Ratio associated with atmospheric turbulence ≤ 50% (goal ≤ 40%).

These requirements apply in the visible (0.5 μm), with a seeing equal to or better than 0.5 arc seconds FWHM. In the following, we define *telescope errors* as all error sources, with the exception of atmospheric turbulence and the accuracy of its correction. The above requirements imply that the telescope errors at science focus must be lower than or equal to 44 nm (goal 35 nm), wavefront RMS. It is fairly evident that such requirements imply that the adaptive optics system must not only compensate for atmospheric turbulence, but also for residual telescope errors. Large amplitude, slowly varying wavefront contributions will have to be removed by active optics.

Active optics will be performed with flexible mirrors of up to 8-m, and typically will have a maximum spatial frequency on the order of 5 cycles per pupil radius. This should be largely sufficient to compensate for manufacturing errors of all monolithic surfaces, as well as slowly varying deflections. Errors with a maximum spatial frequency of ~5 cycles per pupil radius could be allowed to have very large amplitude, possibly up to about 20-50 microns for the lowest modes, a figure which is in-line with the capability of existing active telescopes. A strategy for the control of slowly varying focus and centering is still to be defined.

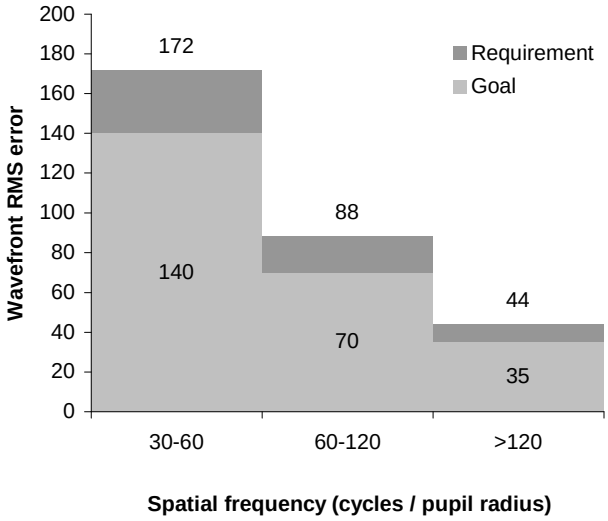

Figure 3. Allowable high frequency wavefront errors (telescope only)

High temporal frequency errors ($\nu \geq 0.1$Hz) and mid-spatial frequency errors will have to be compensated by adaptive optics and should therefore represent only a minor fraction of the phase excursion associated with atmospheric turbulence. Assuming that the adaptive system with the lowest actuator density (the IR adaptive optics module) will have an actuator separation of 80 cm at the entrance pupil, we conclude that at spatial frequencies in the range of 30 to 60 cycles per pupil radius, allowable telescope errors will have to be a few microns at most, possibly ~10 microns peak-to-valley for periods in the 10-m range, with sub-micron accuracy for periods in the 1.6-m range.

Finally, and assuming that the required Strehl Ratio for the telescope errors is the same at all wavelength, and assuming, for example, 3 adaptive systems with actuator separation of 20, 40, and 80 cm respectively (corresponding to r_0=20, 40, and 80 cm), we deduce the maximum high spatial frequency telescope errors (wavefront), as shown in Fig. 3. In brief, the telescope must be diffraction-limited for all error sources having spatial periods below 400 mm.

The requirement for very high spatial frequencies should be easily achieved. For comparison, the high spatial frequency misfigure of the VLT primary mirrors is at least one order of magnitude lower than that specified on Fig. 3.

A source of potential concern, however, is the misfigure of the primary mirror segments. The foreseen size of the segments, 2.3-m diagonal, is fairly close to the adaptive actuator spacing of the IR adaptive system (80 cm in the pupil for correction at ~2 μm and above). The situation improves substantially in the visible, with about 80 actuators per segment area.

In conclusion, the requirement most demanding in terms of telescope errors is probably the image quality at ~2 μm, where the spatial frequency of adaptive correction modes is the lowest. The favorable factor is that, in the spectral range 30-60 cycles per pupil radius, the only significant contributors should be the primary mirror segments. Those will have to be specified to about λ/4 wavefront error RMS to comply with the requirements shown in Fig. 3. This requirement could be substantially relaxed if the adaptive systems could have 1 actuator every ~40 cm in the entrance pupil.

3. Optical design

Two optical designs for the main optics (down to technical field) are briefly outlined below. These designs are associated with specific mechanical structure concepts, and iterations are still in progress.

The first design (Fig. 4), which is the most complex, is constrained to a maximum size of 8.2-m for the corrective optics, i.e. optical substrates for the corrector are monolithic and within demonstrated sizes. The primary mirror focal ratio is f/1.82, the secondary mirror is flat, 33.9-m diameter. Mirror separation is 120.3-m. The four-element corrector includes three aspheric and a flat surface. The design is equivalent to a prime focus design with 3-elements corrector.

The third and fourth mirrors are about 8-m diameter and the fifth mirror is 4.65-m diameter. The fourth mirror has very strong asphericization, with a departure from best fitting sphere on the order of 7-mm. The two other aspheric have departures comparable or lower to that of existing 8-m class mirrors.

The last, flat mirror (M6) can be rotated about the telescope optical axis to direct light to different instruments. With a diameter in the range of 2.5-m, this mirror may be usable for field stabilization at moderate frequencies.

Suppression of stray light associated with the strong spherical aberration is ensured by means of an axial screen located inside the corrector. The central obscuration is essentially determined by the hole in the tertiary mirror. This constraint indirectly limits the available space for the support of the flat folding mirror as well.

The focal ratio at technical focus is f/6.2, a figure that permits off-axis designs of the adaptive module. The technical field of view is 11.7 arc minutes, and limited by the maximum allowable size of the centre hole in the flat relay mirror. Image quality is

excellent, with a diffraction-limited field of view of 3 arc minutes in the visible, significantly exceeding requirements. Distortion is not negligible but rather low (~1% at the edge of the field of view).

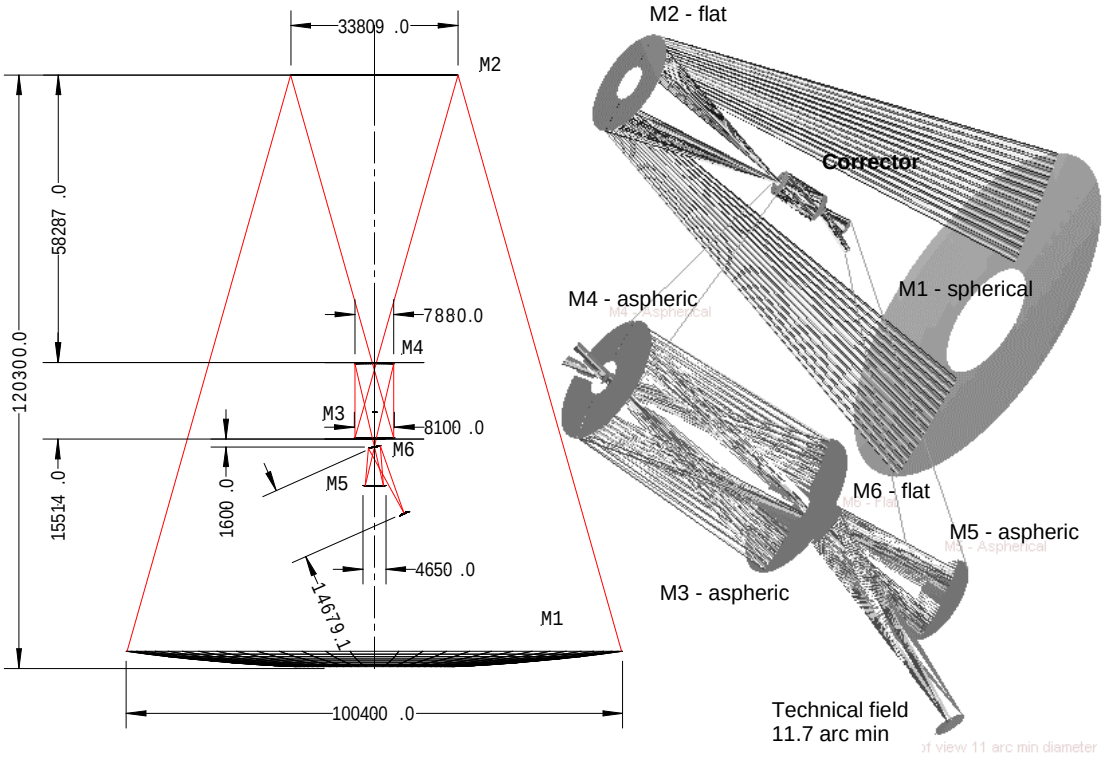

Figure 4. OWL 6-mirror design (all dimensions in m.).

This design has been iterated with one specific concept of the mechanical structure[1]. The obscuration geometry is rather clean and the Point Spread Function fairly close to that provided by a perfect annular aperture (Fig. 5). The location of the corrector above the primary mirror is an advantage with the type of structure envisaged for this optical solution, as it frees space in a critical volume and permits, to some extent, to improve load transfers and tortional stiffness.

A preliminary sensitivity analysis shows that the relative alignment of the mirrors within the corrector is the most critical aspect of this design. A favorable factor is that the structure holding the components of the corrector can be made fairly stiff. The effect of rigid body decenters of the corrector can be well compensated by rotation of the quaternary mirror about its center of curvature, provided that these decenters do not exceed 5-10 mm (lateral) and 10-15 arc seconds (tilt). A strategy for active correction of the effect of decenters is still to be defined, but it is already clear that the number of available degrees of freedom will allow several options.

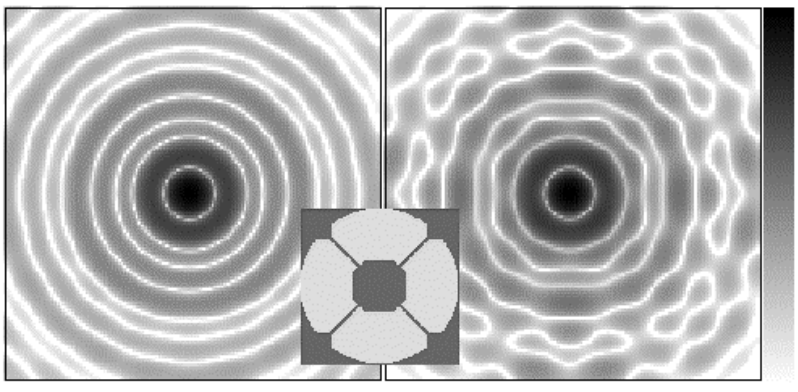

Figure 5. Theoretical Point Spread Function in the visible, logarithmic scale. Left: annular aperture (33% linear obscuration); right: OWL aperture (6-mirror design). The obscuration geometry of the 6-mirror design in the inset.

The second design proposed here is a four-mirror axial system (Fig. 6). Its major drawbacks are the need for a large, 13-m class, monolithic or segmented, aspheric

mirror, and higher field aberrations. It is nonetheless attractive because of the lower number of reflections, and the lower asphericity than in the first design. Conversely, this means that the focal ratio of the primary mirror could be reduced, possibly to ~f/1.50, with a structure height in the range of 100 to 110-m instead of 120-m requested in the 6-mirror design. Compared to the first design, the version presented here has a shorter focal ratio of the primary and the same mirror separation. The possibility to reduce the focal ratio of the primary and thereby structure height is currently being explored.

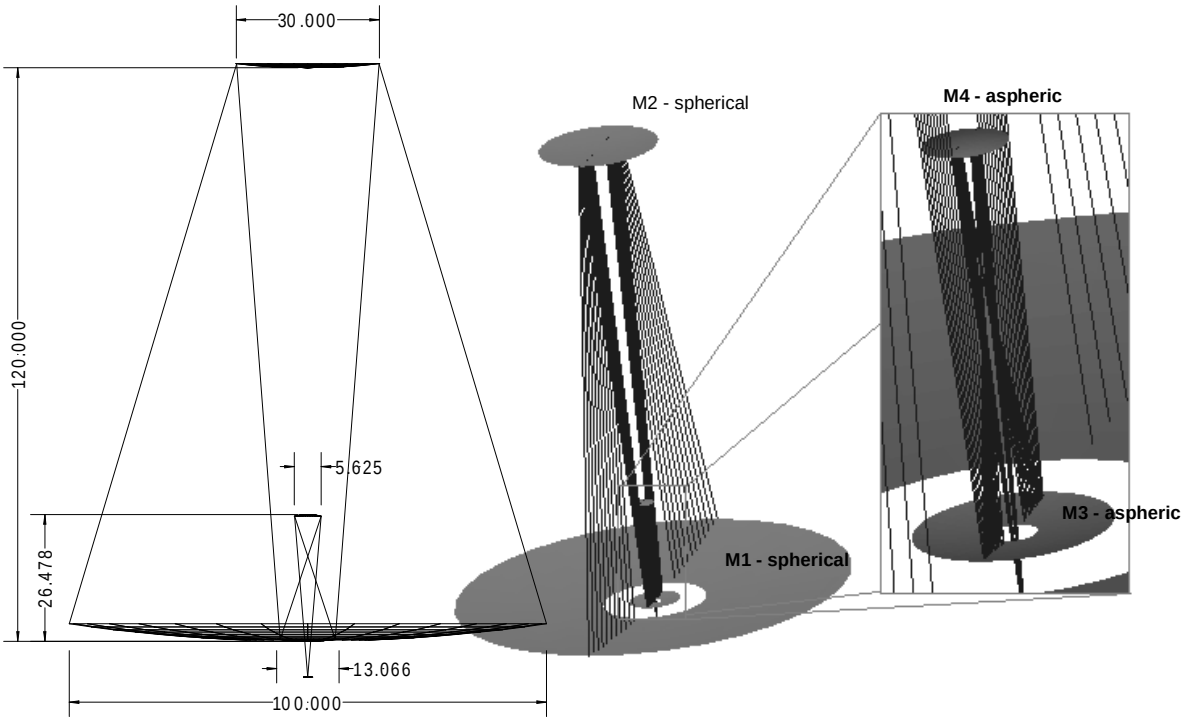

Figure 6. Four-mirror optical design (all dimensions in m.)

The spherical secondary mirror has a diameter of 30 m and compensates a noticeable part of the M1 aperture and field aberrations. There is no intermediate focus between M2 and the corrector, but the actual advantages of an intermediate focus are still to be properly evaluated.

This design is associated with a different structure concept, whereby the mirror M3 is mounted on the M1 structure. Its diameter cannot be reduced because the quaternary mirror is located inside the beam. Since this mirror has to compensate for the major part of the spherical aberration, its diameter cannot be much less than 5 to 6 m. Allowing ~33% obscuration and taking into account the beam diameter at the level of M4, leads to a tertiary mirror diameter of 13 m. This mirror is aspheric with moderate deformation (1.6 mm departure from the best fitting sphere). A monolithic solution might be possible with fused Silica. If not, the mirror would have to be segmented, in which case a 5- or 6- petals configuration would be proposed.

M4 is located at a pupil image and has strong asphericity (~5.6 mm). The intermediate image can probably not be used due to its poor quality and inconvenient location. Baffling is no concern, and the geometry is essentially driven by the central obstruction.

The unvignetted field of view is 11 arc minutes and the telescope focal ratio is f/6.05. The diffraction-limited field of view is 30 arc seconds at 500 nm. The effect of decenters is comparable to that obtained with the 6-mirror design. The reduced number of degrees of freedom should yield a conceptually simpler alignment control. Furthermore, the location of the large tertiary mirror is favorable for centering with respect to the primary mirror. The larger distance between the two mirrors of the corrector, and the limitation on available space for the mounting of the quaternary mirror are however unfavorable in comparison with the 6-mirror design.

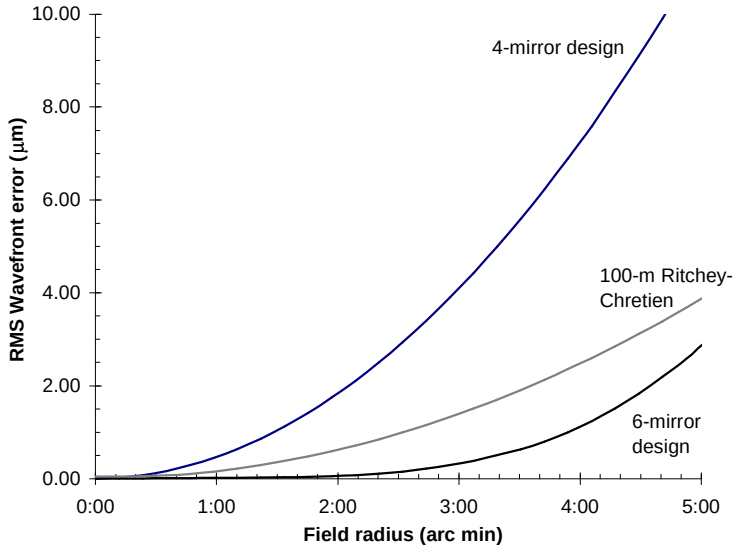

Figure 7. RMS wavefront field aberrations.

Figure 7 compares the RMS field aberrations of the two designs. A 100-m class Ritchey-Chrétien, with 120-m mirror separation, is shown for comparison.

It should be observed that all designs are essentially seeing-limited over the entire (technical) field of view, with images not exceeding 0.2 arc seconds rms for the 4-mirror design.

With three aspheric surfaces, the 6-mirror design provides a performance noticeably superior than an equivalent Ritchey-Chrétien.

The design of the adaptive optics modules is currently in a very early phase. It appears that a general-purpose adaptive module, common to all instruments, would have a prohibitive number of surfaces. The dimensioning requirements include multi-conjugate correction and field of view.

Off-axis designs allow favorable geometries and reduced number of surfaces but require that the input field be well corrected for field aberrations, as virtually no compensation between the axisymmetrical telescope and the asymmetrical adaptive module is possible. This comment applies equally to the 4- and 6-mirror designs, as the last relay mirror is a simple folding flat. Proper correction of the input (technical) field is provided over 30 arc seconds by both telescope designs, but a larger field of view is only properly corrected by the 6-mirror design.

We tentatively assume that adaptive mirrors must be flat and have dimensions in the 0.5- to 2-m range. An example of off-axis design, with 30 arc seconds diffraction-limited field of view, two adaptive mirrors of 1-m class and three relay mirrors is shown in Fig. 8. The relay mirrors are off axis aspheres having a common optical axis. The adaptive mirrors are conjugate to two turbulent layers (altitudes 6 and 10 km, respectively). A second iteration of this design is required to accommodate for re-location of the adaptive mirrors with the variable altitude of the layers. With a lateral magnification layer-mirror in the order of 100, the axial magnification is 10^4 i.e. the mirrors have to translate by 100 mm for 1-km change of layer altitude. Positioning accuracy is not critical (a few mm) in view of the field depth of the conjugation. No attempt has been made so far to optimize the images of the turbulent layers, but the conjugation layer-adaptive mirrors is already fairly good, with a geometrical spot size close to diffraction limit.

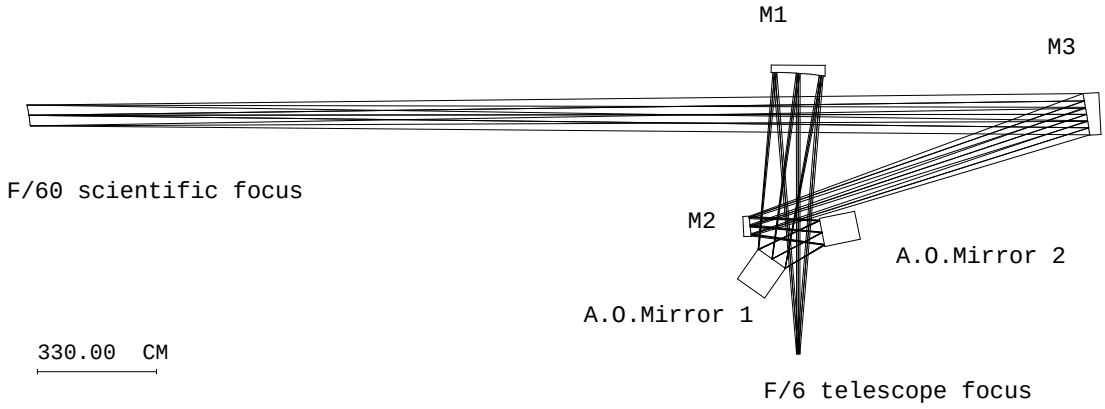

Figure 8. Off-axis adaptive system for 30 arc seconds field of view.

As mentioned in the introduction, it is out of question to transfer the entire technical field of view through the adaptive system. Unless a solution could be found to operate the system in open loop, the only possibility seems to implement pick-off mirrors in the technical field. These mirrors will have to transport images of off-axis reference stars and relocate them into or close to the

science field. This reference beam will have to be tilted in order to simulate the lateral shift of the reference star beam at the level of the atmospheric layers. Vignetting is acceptable, to the extent permitted by the tomographic reconstruction of the atmospheric layers affecting the science field.

4. Active optics and phasing

Wavefront correction is divided in four distinct areas, as function of temporal frequency:

- active correction of large-scale deformations, surfaces misfigure and decenters, to seeing-limited accuracy, at frequencies lower than a few tenth of a Hertz;
- segments alignment and phasing to diffraction-limited accuracy, at frequencies of up to ~1 Hz;
- field stabilization to seeing-limited accuracy, at frequencies of up to ~5Hz;
- adaptive correction of all residual errors, including atmospheric turbulence.

Wavefront sensing for the above corrections is done at technical focus for coarse correction, while fine corrections are deduced from the data produced by the wavefront sensors located within the science field. It is not envisaged to perform active shape control of the primary and secondary mirrors segments.

The principle of active correction, including that of the effect of decenters, can be summarized as follows. Let $Z_i(P)$ be a convenient set of functions describing the observed wavefront at field position P. Assuming reasonable decenters,

$$Z_i(P) = \sum_j \frac{\partial Z_i(P)}{\partial s_j} ds_j + \sum_k Z_{ik}(P) + Z_{i0}(P) \ ,$$

where ds_j are individual decenters, $Z_{ik}(P)$ the wavefront coefficients corresponding to the misfigure of the k=1, …, N reflective surfaces, as seen by the beam corresponding to the field position P, and $Z_i(P)$ corresponds to the design aberrations. Measuring simultaneously the wavefront at a sufficient number of field positions P allows one to invert the above equations and determine the decenters and active shape corrections necessary to restore the condition

$$Z_i(P) = Z_{i0}(P) \ .$$

The system may indeed be over-determined, in which case a least square method provides optimal solution. It should be noted that the field dependency of the effect of surfaces misfigure (terms $Z_{ik}(P)$) is of little concern. First, for each mirror these terms are correlated as they result from the same surface overall misfigure. Second, there is rapid convergence where beam footprint excursion is comparable or lower than the highest spatial period to be corrected. With the VLT, for example, the pupil is on the secondary mirror and the footprint excursion on the primary mirror goes up to about $1/20^{th}$ of the pupil diameter. There is, however, no difficulty in achieving a suitable correction with a single wavefront sensor.

Depending on accuracy requirements, a reduced set of decenters i.e. a limited number of degrees of freedom will most generally be sufficient to perform an acceptable correction. These degrees of freedom are selected according to optical criteria (sensitivities) and mechanical constraints. For a third order correction, and without consideration for surface misfigure, three field positions i.e. three wavefront sensors, would be sufficient. Taking into account the high order terms inherent to OWL design and the number of surfaces, a higher number of wavefront sensors, possibly 5 to 10, may have to be installed at the technical focus. Assuming a sampling in the order of 50×50 or even 100×100, there is little doubt that a sufficient number of stars could be found in the available field of view.

As far as position control is concerned, internal metrology may also be considered if it leads to simplification of the correction scheme.

In the 6-miror design presented above, mirrors M3 to M5, with diameters of 4.65- to 8.2-m, are flexible and monolithic. The flat M6 would most likely be lightweight, with tip-tilt control at a few Hz for field stabilization to sub-arc second accuracy. Active shape control of either M4 or M6 is mandatory (both mirrors being approximately located on an intermediate and on the exit pupil, respectively). Further analysis is required to assess whether M3 or M5 should be actively shape-controlled as well.

In the 4-mirror design, M3 and M4 are flexible, with M4 monolithic and M3 either monolithic or segmented (e.g. four or five petals), and the active mirror would be M4.

Phasing of sub-pupils must be achieved by independent phasing of the primary and secondary mirrors as the field-dependent excursion of the beams footprints is inevitably larger than the gap between segments. At present, we are not aware of any suitable, demonstrated method for piston detection by wavefront sensing. Therefore, we assume that conveniently located position sensors will measure phase errors. This solution has been demonstrated with the Keck telescope, and there is little doubt that the progress of technology should allow even higher performance and lower costs. Finally, there would be no problem to incorporate piston-sensitive wavefront sensors at the technical or science focus, if such sensors would become available. It should be noted, however, that several sensors would be required to alleviate the problem of vignetting and to ensure that the primary and secondary mirrors are independently phased.

With the telescope operating in open air, wind exposure is, in view of the sheer size of the primary and secondary mirrors, a serious issue. Shielding of the primary mirror might be possible to some extent, but it is extremely unlikely that the telescope could be operated on a windy site. Fast tip-tilt actuation of segments would, in theory, be possible, but the technical and financial costs would be too prohibitive. Our estimate is that actuation at more than ~1 Hz will not be practicable. Hence, there will be inevitable restrictions as to the acceptable observatory site and telescope operation.

5. Optical fabrication and testing

Two major challenges underlie the fabrication of the optics of OWL. The first is the production, at an affordable cost and within a reasonable schedule, of the primary and secondary mirror segments. The second is the fabrication of the highly aspheric surface of the compensator.

The primary mirror segments size is still to be finalized, but will most likely be in the 2- to 2.5-m range (diagonal) to permit low transport costs (standard containers) and alleviate the need of active shape control. We will need to produce 1,500 to 2,000 segments within 10 years. The segment thickness envisaged so far is about 100 mm, leading to a total mass of the primary mirror on the order of 1,500-2,000 tons. Secondary mirror segments would be cut to the geometry of groups of 7 primary mirror hexagons, in order to reduce the field-dependent mismatch of segmentation patterns. For evident cost reasons, all segments would be rigorously identical, at the cost of variable gaps and an irregular projection of the segmentation pattern onto the sky.

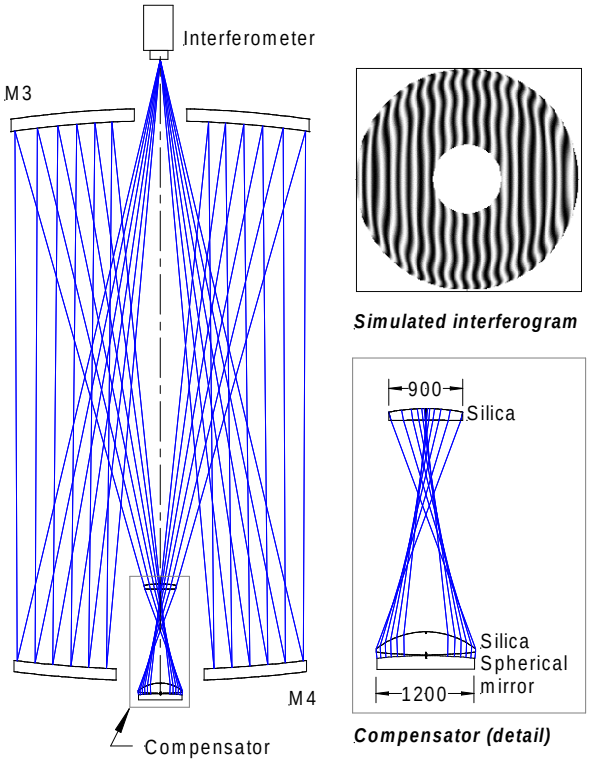

Figure 9. Test set-up for the control of the quaternary mirror (6-mirror telescope optical design). All dimensions are in mm.

Mirror material would be Zerodur, Astro-Sitall, ULE or fused silica. These materials are fully demonstrated in the required sizes, and there is strong confidence that acceptable production rates are possible. Promising developments (currently under evaluation) in the area of silicon carbide substrates may yield substantial savings in mass and noticeable improvements of the mirror supporting mechanisms and telescope structure. There is some confidence that sintered SiC segments in the 2.5-m range could be produced at the desired rate in a cost-effective manner. It remains to be demonstrated, however, that the process could be controlled sufficient accuracy in terms of dimensional predictability, residual stresses, and homogeneity of thermo-mechanical properties.

Assuming sequential grinding, fine grinding and polishing on three 8-m class planetary machines, the primary and secondary mirrors segments can be figured at the requested rate of about one segment every 1.3 days[2]. Round-the-clock operation, which is actually desirable for machine stability, would increase the output rate. The alternative is optical replication, but durability of the master is an issue.

Surface misfigure of individual segments must be negligible at spatial frequencies higher than that corresponding to adaptive correction. As briefly explained in the second section of this article, the requirement

for the primary mirror segments would be about λ/4 wavefront RMS at test wavelength (633 nm) if the correction capability is to be limited by the sampling of the IR adaptive optics system. Unless this requirement could be relaxed, e.g. by constraining the minimum number of adaptive correction modes to that required for visible or very near-infrared correction, it seems mandatory that provision be made for at least one ion-beam figuring machine, to finish off segments which would not meet the requirements after polishing on planetary machines. Warping harnesses would also allow some relaxation of segments misfigure, at the cost of added support complexity.

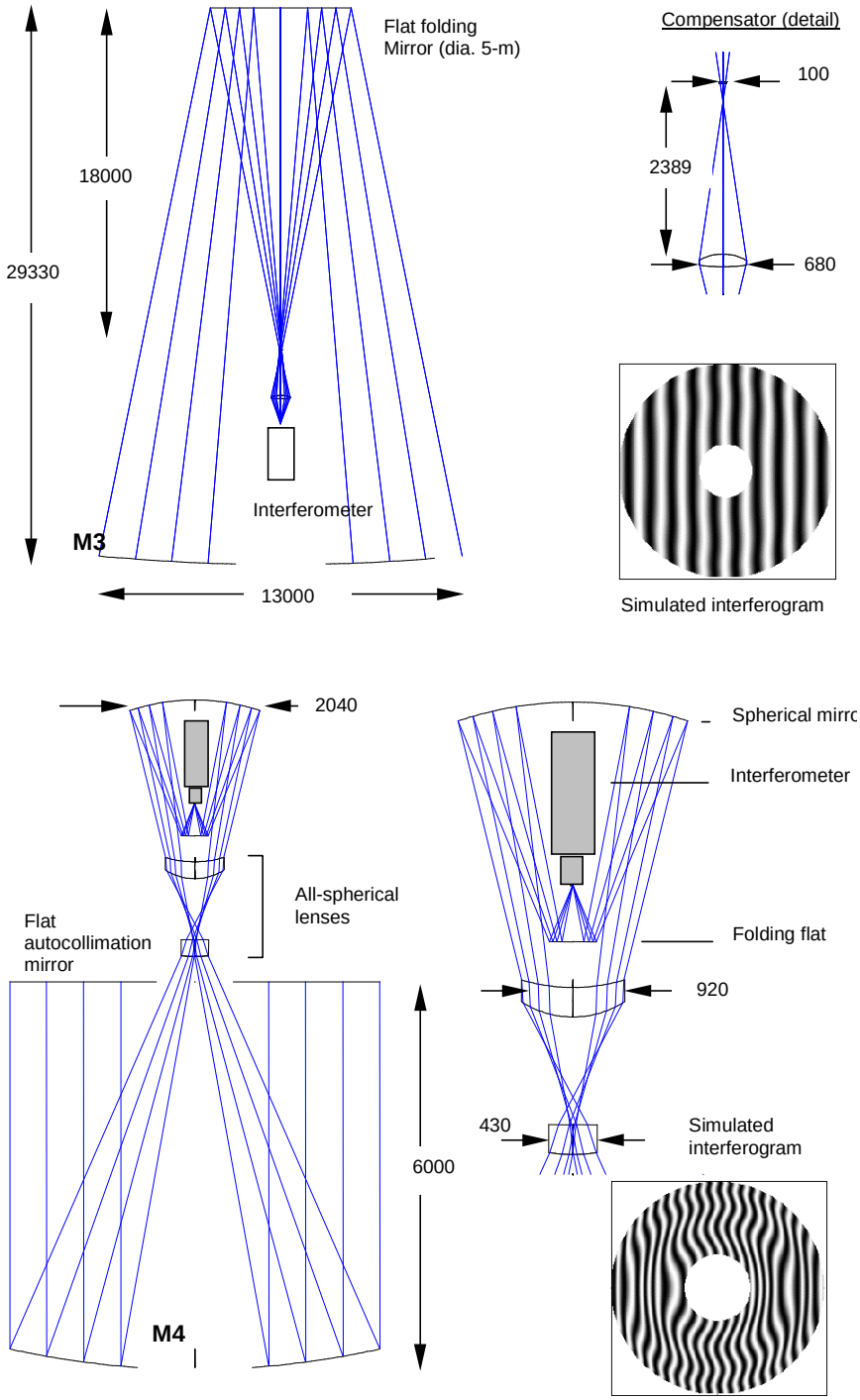

Figure 10. Optical test set-up for M3 and M4, 4-mirror telescope design (all dimensions in mm)

The second challenge is the production of the aspheric surfaces. In the 6-mirror design, mirrors M3 and M5 have deviations comparable to or less than that of existing 8-m mirrors, while M4 has a deviation from best fitting sphere on the order of 7-mm. However spectacular such deviation may seem, there is strong confidence that the surface could be generated by computer-controlled polishing techniques, provided that the surface can be measured. For evident reasons, we give preference to optical set-ups with all-spherical compensators, and allowing full-pupil measurement. A possible solution, shown in Fig. 9, requires the tertiary mirror to be produced first, and then mounted concave side down, about 15.4-m above the polishing machine. A compensator made of two spherical lenses and a spherical autocollimation mirror is mounted at the level of the quaternary mirror, which is measured in double pass. A simulated interferogram is shown in Fig. 9. Compensation is not perfect, but residuals can be calibrated and are sufficiently low so at to not impair measurement accuracy. Calibration of the compensator errors will imply stringent requirements on the measurement of components, but this appears to be achievable.

Centering tolerances are inevitably tight, in the 0.01 to 0.05 mm range. Filtering of the effect of the set-up decenters by measuring the wavefront at several azimuthal orientations of the mirror under test, as demonstrated with the VLT primary mirrors[3], will probably be required.

As for mirrors M3 and M6, the asphericity is

low and the radii of curvature below 30-m. Optical test set-up is comparable to and possibly simpler than those used for the production of the current generation of 8-m mirrors.

In the 4-mirror design, deviations of the aspheric mirrors are in the 1.6 and 5.6-mm range, respectively. Mirror M3 can be tested at the center of curvature through a 2 lens compensator (Fig. 10, upper part). Mirror M4 would have a more complex test set-up, with two lenses, 920 and 430 mm, respectively, a 2-m class spherical mirror and a 5.6-m autocollimation flat (Fig. 10, lower part). This autocollimation flat could also be used to reduce test tower height for the testing of M3, as shown in Fig.10.

Alternatively, Computer-Generated Holographic (CGH) compensators[5] could most likely lead to substantial simplification of the set-ups described above.

With the aspheric mirrors, an alternative to aspheric polishing could be to apply a suitable force distribution and polish the mirrors spherical. The force distribution corresponding to the aspherical deformation can be applied in situ in the telescope if the mirror is polished spherical on a uniform force distribution. Alternatively, the force distribution can be applied during the spherical polishing, the required aspherical figure being obtained when forces are released. For highly aspherical optics like those considered in optical designs presented here, the second solution is preferred as it yields low stresses in the mounted mirror. This method, also known as *stress polishing*, is directly derived from elastic relaxation theory and since the first corrector plate was made by B. Schmidt (1932) numerous studies have been carried out, leading to the realization of small and medium size highly aspherical optics.

Two classes of mirrors can be considered for elastic relaxation methods, depending whether the thickness distribution is constant or radially variable. The variable thickness distribution solution is the most interesting as it requires a uniform force distribution during polishing to produce the aspherical shape. The thickness profile of the mirror before spherical polishing is calculated according to the final figure and the stress applied.

First calculations show that for a 6-8 m class mirror with the high asphericity foreseen in the OWL designs, and considering a uniform load during polishing in the range of 0.04 to 0.08 MPa, the central thickness of the mirror would be in the 65 to 80mm range (assuming Zerodur). Using metal alloys with a higher elastic limit, this figure could be reduced to 50 to 60mm. However, this would increase stresses during polishing and could result in unacceptably high, uncontrolled relaxation.

The realization of the highly aspheric optic of OWL is a technical challenge for optical manufacturing, as elastic relaxation methods have never been used on such large mirrors. Relatively higher deformations have been already generated but on small or medium size mirrors. Nevertheless, we are confident that further investigations, taking into account the necessary active support of such a thin meniscus, will lead to a feasible concept. It should be observed that, under the reasonable assumption that stress relaxation would not lead to high spatial frequency errors, spherical stress-polishing is potentially the most attractive solution in terms of surface smoothness.

In view of the requirements discussed in section 2, and no matter which design is selected, the optical quality specifications of all monolithic mirrors would be divided in three parts:

1. Lowest spatial frequency modes, up to ~5 cycles per pupil radius. In this range, relaxation is permitted by active optics. The most convenient specification would be the allowable range of active correction forces. For reference, the misfigure of the VLT primary mirrors is in the range of a few microns, and corrected with peak forces in the range of ~80 N.
2. Intermediate frequency range, up to ~30 cycles per pupil radius. In this range, correction must be performed by the adaptive optics system. A possible specification would be based on the Power Spectral Density of the misfigure, allowing, for example, a few microns at 5 cycles per pupil radius, down to sub-micron accuracy at 30 cycles per radius. For reference, the misfigure of the VLT primary mirrors in this spatial frequency range is in the order of 35-40 nm wavefront RMS, i.e. substantially better than required with OWL.
3. High spatial frequency range, above 30 cycles per pupil radius. No correction being possible, residual errors would have to be well within the limits specified in section 2, shown in Fig. 3. Taking into consideration the fact that the VLT 8-m primary mirrors are at least one order of magnitude better than these limits, the high spatial frequency requirements should not be an issue.

Optical testing aside, we conclude that the aspheric surfaces of OWL may not represent a much greater challenge than the fabrication of VLT mirrors. Higher costs and longer lead-times are however to be expected, in view of the complexity of the optical test set-ups and, possibly, of the need to manufacture M3 and M4 sequentially.

6. Conclusions

We are confident that design and fabrication solutions for the optics of the OWL telescope exist and do not require substantial extrapolation of present-day technologies. With the exception of adaptive optics, the challenge we face is lower than that of the fabrication of the Keck and VLT optics one-decade ago, which required substantial R&D in optical fabrication. Initial cost and lead-time estimates[2] remain the same, and are still deemed conservative.

We have identified at least two optical design solutions. The 6-mirror solution provides an optical performance superior to that of an equivalent Ritchey-Chrétien system, and has very favorable properties with respect to static deformation of the giant telescope structure and the implied tolerances on mirrors decenters. A 4-mirror solution is currently being iterated for optical performance and feasibility. Early results indicate that this solution may allow a noticeable reduction of structure height, but further analysis is required to verify that the solution can meet all requirements, including feasibility of test set-ups for optical fabrication.

Mass-production of mirror substrates is fully compatible with existing, proven processes. Optical fabrication on planetary machines, complemented with ion-beam finishing, has been demonstrated with the Hobby-Eberly project[5]. There is very strong confidence that the process could be adapted to the production of OWL primary and secondary mirrors. Fabrication of the highly aspheric surface of the corrector imposes a rather complex test set-up, but surfacing would be somewhat easier than with current 8-m class mirrors, due to tolerance relaxation.

The critical area is adaptive optics, where substantial effort must be put in establishing an acceptable multi-conjugate solution, and in identifying realistic mirror and wavefront sensing technologies.

7. References

1. E. Brunetto et al, this conference.
2. R. Gilmozzi et al, *The future of filled aperture telescopes: is a 100m feasible?*, SPIE 3352, pp. 778-791.
3. P. Dierickx et al, *VLT Primary Mirrors: mirror production and measured performance,* 1996, SPIE 2871, pp. 385-392.
4. J. H. Burge, *Advanced Techniques for Measuring Primary Mirrors for Astronomical Telescopes*, 1993, Ph.D. dissertation.
5. F. Carbone, *Innovations make large-segment-mirror telescopes more affordable*, Laser Focus World, Aug. 1998, 229.

Submitted at the *Workshop on Extremely Large Telescopes*, Bäckaskog, Sweden, June 1-2, 1999.